Geophysical Research Letters

RESEARCH LETTER
10.1029/2019GL082838

Oceanic Drivers of Widespread Summer Droughts in the United States Over the Common Era

Seung H. Baek[1,2], **Nathan J. Steiger**[1], **Jason E. Smerdon**[1], **and Richard Seager**[1]

[1]Lamont-Doherty Earth Observatory, Columbia University, Palisades, NY, USA, [2]Department of Earth and Environmental Sciences, Columbia University, New York, NY, USA

Key Points:
- Widespread summer droughts in the contiguous United States have been endemic over much of the Common Era based on a new paleo data assimilation product
- La Niñas are the principal driver of these widespread droughts, while the Atlantic is shown to have played a passive role
- The oceanic drivers of these droughts over the paleo record is consistent with previous model-based findings over the instrumental record

Supporting Information:
- Supporting Information S1

Correspondence to:
S. H. Baek,
sbaek@ldeo.columbia.edu

Citation:
Baek, S. H., Steiger, N. J., Smerdon, J. E., & Seager, R. (2019). Oceanic drivers of widespread summer droughts in the United States over the Common Era. *Geophysical Research Letters*, *46*, 8271–8280. https://doi.org/10.1029/2019GL082838

Received 14 MAR 2019
Accepted 3 JUL 2019
Accepted article online 8 JUL 2019
Published online 18 JUL 2019

Abstract We examine oceanic drivers of widespread droughts over the contiguous United States (herein pan-CONUS droughts) during the Common Era in what is one of the first analyses of the new Paleo Hydrodynamics Data Assimilation (PHYDA) product. The canonical understanding of oceanic influences on North American hydroclimate suggests that pan-CONUS droughts are forced by a contemporaneous cold tropical Pacific Ocean and a warm tropical Atlantic Ocean. We test this hypothesis using the paleoclimate record. Composite analyses find a robust association between pan-CONUS drought events and cold tropical Pacific conditions, but not with warm Atlantic conditions. Similarly, a self-organizing map analysis shows that pan-CONUS drought years are most commonly associated with a global sea surface temperature pattern displaying strong La Niña and cold Atlantic Multidecadal Oscillation (AMO) conditions. Our results confirm previous model-based findings for the instrumental period and show that cold tropical Pacific Ocean conditions are the principal driver of pan-CONUS droughts on annual timescales.

Plain Language Summary Widespread summer droughts across the contiguous United States (pan-CONUS droughts) pose unique challenges because of their potential to strain multiple water resources simultaneously, and the financial damages from these droughts are significant. For example, pan-CONUS droughts in 1988 and 2012 cost an estimated $40 and $30 billion, respectively. We provide a millennium-length perspective on the causes of these droughts using a new paleo reconstruction product that merges climate model information with multiple climate proxies including tree rings, ice cores, and corals. We characterize pan-CONUS droughts from 850 to 1850 CE and demonstrate how ocean variability has helped cause these events. We find that La Niña events in the tropical Pacific are the principal oceanic influence on these droughts, while variability in the Atlantic has not played a significant role. These findings are at odds with previous work that has estimated a role for the Atlantic in causing pan-CONUS droughts but support conclusions from a more recent model-based study of the causes of pan-CONUS droughts over the instrumental record. Our findings are important for predictions of pan-CONUS droughts and for determining how the occurrence of these droughts may change in the future due to increases in greenhouse gas emissions.

1. Introduction:

Seasonal droughts that span most of the contiguous United States (herein pan-CONUS droughts) are a prominent feature of North American hydroclimate. Because of their extensive spatial coverage and potential to strain multiple water and agricultural resources simultaneously, pan-CONUS droughts pose unique mitigation challenges that can lead to disproportionately high economic costs. For instance, the 1988 and 2012 U.S. droughts ranked among the most spatially extensive in recent history (Andreadis et al., 2005; Kogan, 1995; National Climatic Data Center, 2013; Trenberth et al., 1988) and cost a respective U.S. $40 and $30 billion, largely in agricultural losses (Rippey, 2015). Although pan-CONUS droughts are consistently observed in the paleoclimate and instrumental record (Cook et al., 2014) and replicated in model simulations (Baek et al., 2019; Coats et al., 2015), characterizing their causes remains a challenge because they span multiple regions with distinct climates and varying sensitivities to ocean forcings.

The canonical understanding of oceanic influences on U.S. hydroclimate (Hoerling & Kumar, 2003; McCabe et al., 2004; Schubert et al., 2009) would suggest that pan-CONUS droughts are strongly associated with contemporaneous cold tropical Pacific and warm tropical Atlantic sea surface temperatures (SSTs). Cold phases of the El Niño Southern Oscillation (ENSO; or La Niñas) and Pacific Decadal Oscillation (PDO) establish an atmospheric ridge over the northern Pacific that diverts subtropical jets northward (Sarachik & Cane, 2010;

Seager et al., 2005; Trenberth & Guillemot, 1996), while warm phases of the Atlantic Multidecadal Oscillation (AMO) are hypothesized to weaken the North Atlantic Subtropical High that in turn suppresses summertime low-level jets and the North American Monsoon (Hu et al., 2011; Hu & Feng, 2012; Kushnir et al., 2010; Nigam et al., 2011; Oglesby et al., 2012), all of which cause broad precipitation deficits over various regions of the United States. The above Pacific and Atlantic states have been shown to influence pan-CONUS droughts over the observational interval (e.g. Coats et al., 2015; Cook, Smerdon, Seager, & Cook, 2014), but multidecadal variability in both the Pacific (e.g. Cobb et al., 2003, 2013; Lu et al., 2018; Wittenberg, 2009) and Atlantic basins (e.g. Wang et al., 2017) remains poorly characterized by the limited ~150-year observational interval.

Limited sampling of pan-CONUS droughts provided by the short observational interval, and the influence of stochastic internal atmospheric variability (e.g. Ault et al., 2018; Baek et al., 2019; Bishop et al., 2019; Cook et al., 2018; Seager & Hoerling, 2014; Williams et al., 2017), makes it difficult to fully characterize how atmospheric and oceanic variabilities combine to cause such events. To circumvent these challenges, Baek et al. (2019) used ensembles of atmospheric model runs forced with observed SSTs (i) over the global ocean, (ii) over the tropical Pacific Ocean only, and (iii) over the tropical Atlantic Ocean only. This approach (e.g. Kushnir et al., 2010; Seager et al., 2005) not only provided multiple realizations of atmospheric responses to SST conditions over the observational interval (1856-2012) but also isolated the influence of Pacific and Atlantic Ocean conditions on pan-CONUS droughts. Baek et al. (2019) concluded that pan-CONUS droughts were forced by cold states of the tropical Pacific and internal atmospheric variability but not by warm states of the tropical Atlantic. These findings are nonetheless in contrast with expectations from previously identified associations between Atlantic conditions and spatially widespread droughts over North America (e.g. Coats et al., 2015; Cook, Smerdon, Seager, & Cook, 2014).

In this study, we examine the causes of pan-CONUS droughts since 850 CE in one of the first analyses of the new Paleo Hydrodynamics Data Assimilation product (PHYDA; Steiger et al., 2018), which uses a data-assimilation framework to merge 2,978 paleoclimatic proxies with the National Center for Atmospheric Research (NCAR) Community Earth System Model (CESM) Last Millennium Ensemble (Otto-Bliesner et al., 2016). The PHYDA allows a more thorough, wide-ranging, and comprehensive analysis of the causes of pan-CONUS droughts than was previously possible by placing these events in the regional, hemispheric, and global atmosphere-ocean context of the last thousand years or more.

2. Data and Methods

We use the Palmer Drought Severity Index (PDSI) and 2-m surface air temperature outputs from a 100-member ensemble of the PHYDA. PDSI is a normalized index of soil moisture, with a persistence of 12-18 months (e.g. Palmer, 1965), that is calculated using a simple moisture-balance model of precipitation and potential evapotranspiration (using the Penman-Monteith formulation; Steiger et al., 2018). Two-meter surface air temperature provides near-surface temperature globally and is interpreted as representative of SSTs on seasonal and annual timescales herein. We use boreal summer (June-July-August [JJA]) averages of PDSI. We use boreal summer and boreal winter (December-January-February [DJF]) averages of SST anomalies. SST anomalies are derived by centering SST at each grid point relative to its climatological mean from 850 to 1850. All PHYDA outputs span the years 1-2000 CE on a 2.5° latitude by ~1.9° longitude grid resolution.

To evaluate the representation of pan-CONUS droughts in the PHYDA, we employ the Living Blended Drought Atlas version of the North American Drought Atlas (NADA; Cook et al., 2010). The NADA reconstructs PDSI estimates from tree-ring chronologies and has been widely analyzed to understand drought history and dynamics over North America (see the reviews in Cook et al., 2007, and Cook et al., 2016), including pan-CONUS droughts over the last millennium (Cook, Smerdon, Seager, & Cook, 2014). PDSI from the NADA is available as JJA averages, thus consistent with the JJA PDSI averages used from the PHYDA. The NADA spans the period 1–2005 CE with an even latitude-longitude grid resolution of 0.5°. Although data from both the PHYDA and NADA span the full Common Era, we focus our analyses on the 850–1850 CE interval. We use 850 CE as the lower bound to ensure sufficient availability of proxy coverage over the CONUS domain and 1850 CE as the upper bound to remove intervals widely affected by anthropogenic forcings.

Lastly, we employ volumetric soil moisture from a 16-member SST-forced ensemble of the NCAR Community Atmosphere Model 5 (CAM5; Hurrell et al., 2013) forced by global SSTs from 1856 to 2012. Outputs from CAM5 are provided on an ~2.8° grid. We take JJA averages of modeled volumetric soil moisture at 80-cm depth (linearly interpolated) and standardize the variable by subtracting and dividing by its 1856–2012 mean and standard deviation, respectively. The SSTs from the CAM5 simulations are centered by subtracting the local 1856–2012 mean from each grid point. The standardized JJA volumetric soil moisture and centered SSTs are linearly detrended to remove the largest influences associated with anthropogenic warming.

We focus on a region approximately encompassing the CONUS (24.5–49°N, 59.5–127°W). We define pan-CONUS droughts as years in which at least 50% of the regional area includes PDSI or standardized volumetric soil moisture with half a standard deviation or more below the climatological mean. Prior investigations of pan-CONUS droughts over North America (e.g. Coats et al., 2015; Cook, Smerdon, Seager, & Cook, 2014) have used a different definition requiring spatial averages over three or four regions (American Southwest, Central Plains, Northwest, and Southeast) to be in drought, but we depart from this precedent to allow all areas within the CONUS domain to contribute to pan-CONUS drought occurrence. Our definition selects for a larger number of pan-CONUS droughts because of the additional areas included, but the two definitions yield similar spatial patterns in their composites (not shown). We composite pan-CONUS drought years across (i) a 100-member PHYDA ensemble from 850 to 1850, (ii) the NADA from 850 to 1850, and (iii) the 16 CAM5 simulations of the 1856–2012 period. SST anomalies during pan-CONUS drought years are also composited for the PHYDA and the CAM5 ensembles, respectively. The years composited are selected solely on the basis of the pan-CONUS drought criterion; we do not consider drought variability on other continents nor SSTs from any region in our selection.

We use the monthly NINO3.4 and the seasonal North Atlantic Sea Surface Temperature (NASST) indices reconstructed in the PHYDA to characterize the state of the Pacific and Atlantic, respectively. The NINO3.4 index in PHYDA is defined as the monthly average SST anomaly of the region bounded by 5°N-5°S, 170°-120°W, from which we use the DJF average. The NASST index is defined as the JJA average SST anomaly of the region bounded by 0°–60°N and 0°–80°W. The boreal winter and summer months are chosen to reflect the dominant season of ENSO (Rasmusson & Carpenter, 1982; Stein et al., 2014) and AMO (Enfield et al., 2001) influences, respectively. To evaluate the influences of ENSO and AMO on the spatial extent of drought over the United States, the percent of CONUS under drought (calculated by dividing the number of grid cells under drought by the total number of grid cells) is determined during La Niñas and warm AMO events and is compared against the percent of CONUS under drought during all years. We define La Niña (warm AMO) events as years when the NINO3.4 (NASST) index is half a standard deviation or more below (above) the 850–1850 mean. Significant differences between distributions are determined using the Kolmogorov-Smirnov test (Chakravarti et al., 1967).

We conduct an 8-node self-organizing map (SOM) analysis on the detrended and area-weighted April-to-March annual SST field for the ensemble mean of the PHYDA (Kohonen, 1998). The SOM analysis is an unsupervised artificial neural network technique that compresses a high-dimensional data field into a lower dimensionality while preserving neighborhood topology (Liu et al., 2006). It is analogous to empirical orthogonal function analysis, which decomposes the data field into leading orthogonal covariance patterns, but unlike empirical orthogonal function analyses does not impose linearity or orthogonality (Steiger et al., 2018). After computing the SOM nodes, the algorithm also classifies the SST field of each year according to the node that it matches best (the "best matching unit"; herein BMU) according to the shortest Euclidean distance between the SST fields and the SOM nodes. PDSI fields are composited across the years that correspond to the BMUs of each SOM.

3. Results

Figure 1a shows boxplots of the distribution in the number of pan-CONUS droughts estimated per century by the 100-member PHYDA ensemble from 850 to 1850 (the last "century" has 101 years because it includes 1850) and the corresponding number of pan-CONUS droughts recorded in the NADA. Because each member of the PHYDA is a separate realization of atmospheric responses that are constrained by the same proxy network, the 100-member ensemble represents 100 estimates of the number of pan-CONUS droughts. The

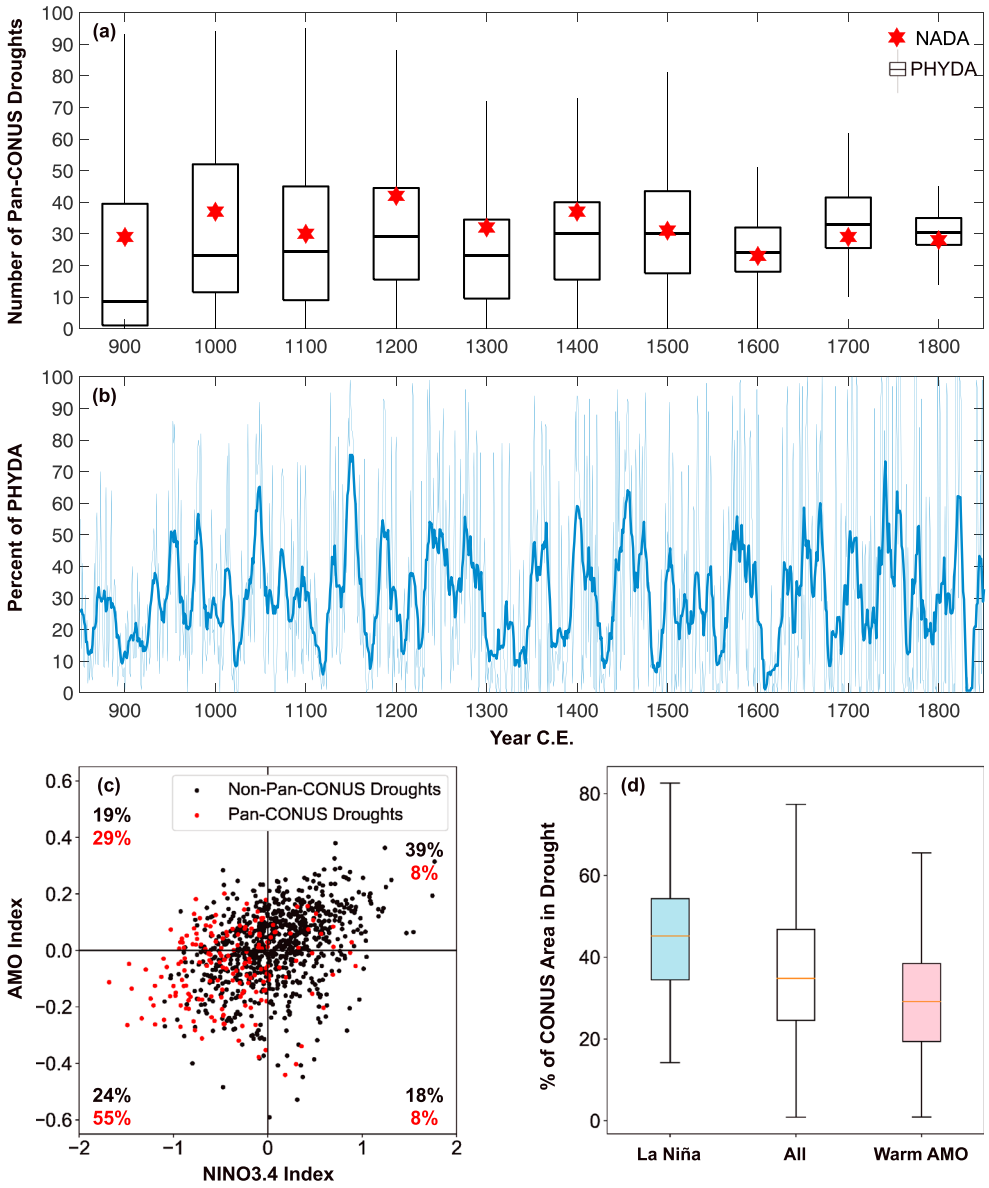

Figure 1. (a) Pan-contiguous United States (CONUS) drought occurrences in the PHYDA and NADA. Boxplots represent the distribution of the number of pan-CONUS droughts estimated per century by the 100-member PHYDA ensemble. Years on the *x* axis represent the center year during a 100-year period over which the distributions were calculated. (b) Time series of the percent of the 100-member PHYDA ensemble that estimate pan-CONUS droughts in a given year. Annual values are represented in light blue; the thick blue line is a 10-year moving average. (c) NINO3.4 index and NASST index values for pan-CONUS droughts and all other years from 850–1850. Percentages represent the number of years in which pan-CONUS (red) and non-pan-CONUS (black) droughts fall in each of the four respective quadrants. (d) Boxplots of the percent of CONUS in the PHYDA under drought during (i) La Niña years, (ii) all years, and (iii) warm AMO years over the period 850–1850.

number of pan-CONUS droughts per century recorded in the NADA falls within the 25th and 75th percentiles of the distribution estimated by the 100-member PHYDA ensemble, suggesting that the PHYDA estimates the incidence of pan-CONUS droughts in a manner consistent with the more widely analyzed and assessed NADA product. To visualize the distribution of pan-CONUS droughts in a more continuous manner, Figure 1b shows a time series of the percent of the 100-member PHYDA ensemble that estimates pan-CONUS droughts in each year.

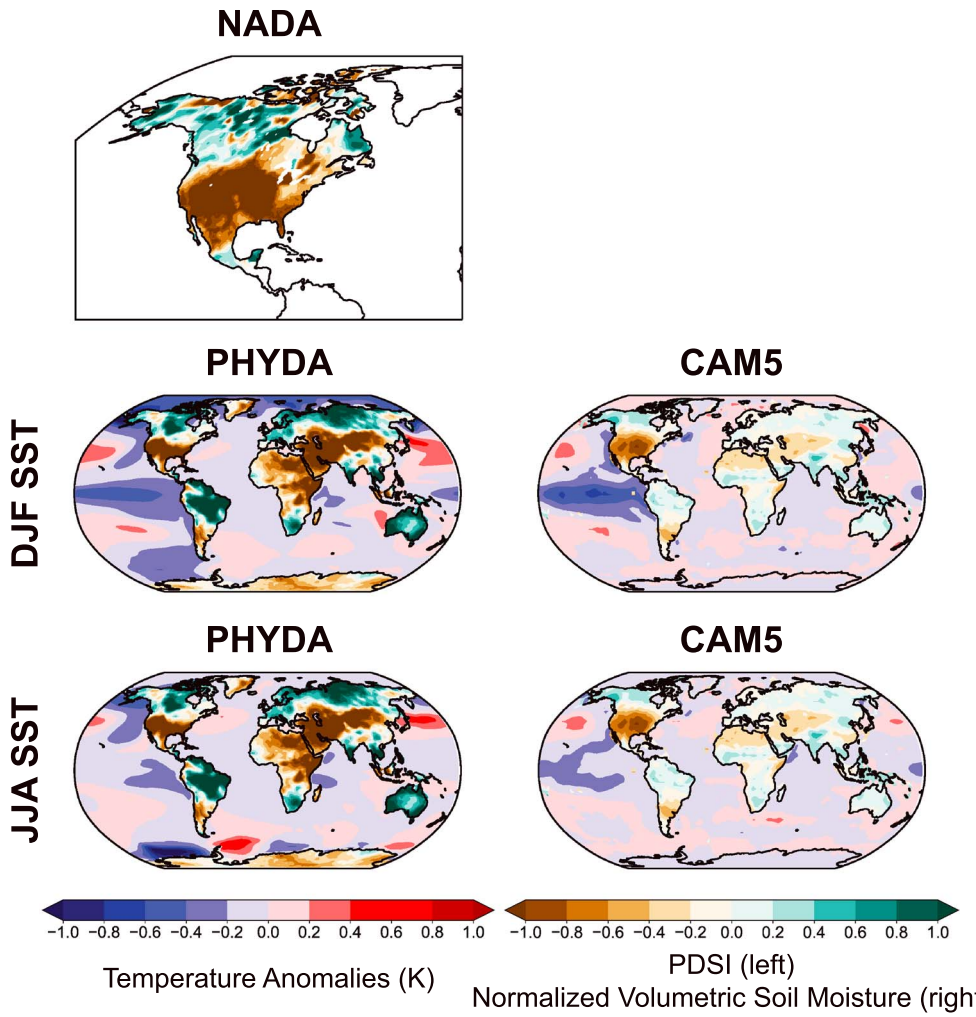

Figure 2. Composites of pan-contiguous United States (CONUS) droughts in the North American Drought Atlas (NADA; 850-1850), across the 100-member Paleo Hydrodynamics Data Assimilation (PHYDA) ensemble (850-1850), and in the Community Atmosphere Model 5 (CAM5) sea surface temperature (SST)-forced ensemble (1856-2012). In all maps the June-July-August (JJA) Palmer Drought Severity Index (PDSI; NADA and PHYDA) or normalized volumetric soil moisture (CAM5) is composited, while the DJF and JJA SST fields are composited separately for both the PHYDA and the CAM5 ensembles. The numbers of events in the composites are 318, 34,230, and 303 for NADA, PHYDA, and CAM5, respectively.

To first characterize the influence of La Niñas and warm AMO events on pan-CONUS droughts in PHYDA, Figure 1c plots NINO3.4 and NASST index values for (i) pan-CONUS drought years and (ii) all years that do not include pan-CONUS droughts. Pan-CONUS droughts indicate a clear tendency toward negative values of both NINO3.4 and NASST indices, as over half of all pan-CONUS droughts have negative NINO3.4 and NASST values (and 84% of pan-CONUS droughts have negative NINO3.4 values). To further characterize the noted associations, boxplots of the percent of CONUS in the PHYDA under drought during (i) all years, (ii) La Niña years, and (iii) warm AMO years over the 850–1850 interval are plotted in Figure 1d. Relative to all years, the percent of CONUS under drought increases significantly during La Niñas but decreases significantly during warm AMO events ($p<0.05$). As with the scatter plot in Figure 1c, the increase in the spatial extent of drought during La Niñas is expected, but the decrease in the spatial extent of drought during warm AMO events is surprising. The absence of an increase in the spatial extent of droughts during warm AMO events is nonetheless consistent with the modeling studies of Baek et al. (2019), who also found the percent of CONUS under drought to decrease during warm AMO events.

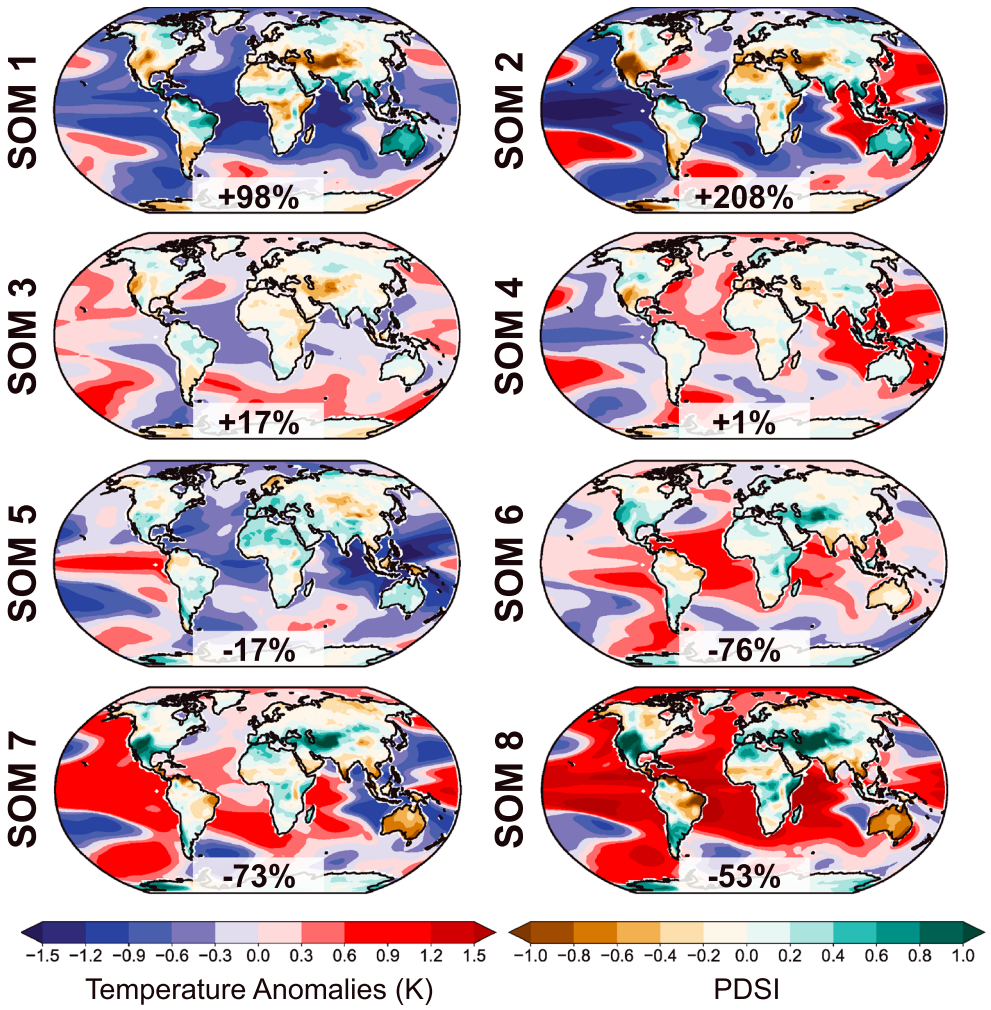

Figure 3. The eight-node patterns from the self-organizing map (SOM) analysis of the Paleo Hydrodynamics Data Assimilation (PHYDA) sea surface temperature (SST) fields and the associated global Palmer Drought Severity Index (PDSI) patterns composited over best matching unit (BMU) years of each SOM. The percent change in BMU frequency during pan-contiguous United States (CONUS) drought years, relative to non-pan-CONUS drought years, is given in the bottom of each SOM map.

Figure 2 plots composites of PDSI during pan-CONUS droughts for (i) the NADA from 850 to 1850, (ii) the 100-member ensemble of the PHYDA from 850 to 1850, and (iii) the 16-member CAM5 ensemble from 1856 to 2012, with the PHYDA and CAM5 composite maps including global SST anomalies for the DJF and JJA seasons (all plots show JJA PDSI or soil moisture values). The three composites show widespread spatial agreement over North America, as exhibited by broadly dry and wet conditions over CONUS and continental Canada, respectively. For the PHYDA and CAM5, this spatial agreement extends to most of the globe, although the magnitude of the wet and dry anomalies globally is more pronounced in the PHYDA composite likely because of the far greater number of drought events sampled (N = 34,230) relative to those in the CAM5 composite (N = 303). The SST anomalies composited over PHYDA and CAM5 also show significant spatial similarities—both composites display patterns characteristic of canonical La Niña and cold PDO conditions in the Pacific and largely neutral conditions in the Atlantic. These ocean states are reflected in the mean values of the NINO3.4 and NASST indices during pan-CONUS drought years in the PHYDA (CAM5), which are -0.40 (-0.56) and -0.06 (-0.05), respectively.

To further evaluate the association between pan-CONUS droughts and the identified ocean states, we use the described SOM analysis of the global SST field from PHYDA. Contrary to our preceding composite analyses that rely on the identification of pan-CONUS droughts and the analyses of the corresponding ocean

Table 1
The Percent (%) and Total Number of Years (#) That Each Respective Node Claims as the BMU for Pan-CONUS Drought Years and Non-pan-CONUS Drought Years

SOM	% (#) Pan-CONUS drought years	% (#) Non-pan-CONUS drought years
1	19 (35)	10 (79)
2	28 (51)	9 (74)
3	18 (33)	15 (126)
4	14 (26)	14 (115)
5	8 (14)	9 (75)
6	4 (8)	18 (149)
7	4 (7)	14 (114)
8	5 (9)	11 (86)

Note. Abbreviations: BMU, best matching unit; CONUS, contiguous United States.

conditions, the SOM analysis is independent of any assumptions about the hydroclimate states over land. Figure 3 maps the eight SOM node patterns of global SST; included in the maps is the corresponding global PDSI field composited over the years in which a given node is the BMU. The percent and total number of years that each respective node is the BMU for pan-CONUS drought years and non-pan-CONUS drought years is given in Table 1. The percent change in BMU frequency for each node from years that do not include a pan-CONUS drought to years that do is provided in the bottom of each node pattern map.

SOMs 1–4 show La Niña-like patterns, while SOMs 5–8 show El Niño-like patterns. SOMs exhibiting La Niña-like (El Niño-like) patterns increase (decrease) in BMU frequency during pan-CONUS drought years relative to non-pan-CONUS drought years. SOMs with the strongest La Niña patterns (SOMs 1 and 2) furthermore lead to the greatest increases in BMU frequency (+98% and +208%, respectively). While SOMs with cold (warm) Atlantic conditions generally show increases (decreases) in BMU frequency, the state of the Atlantic does not seem to have nearly as strong of an influence in BMU frequency changes as the Pacific. For instance, although SOM 8 has by far the warmest Atlantic conditions, it shows smaller decreases in BMU frequency (-53%) than SOMs 6 and 7 (-73% and -75%, respectively), both of which exhibit more modest warm Atlantic conditions. Similarly, despite widespread warming over the north Atlantic and concurrently modest La Niña conditions, SOM 4 shows only a 1% increase in BMU frequency. We also note that while there is no objective method to determine the appropriate number of SOM nodes, we have selected the number of SOMs that roughly maximizes the number of different global SST patterns generated before the patterns become redundant. Our collective results are nevertheless unchanged in analyses that include 6 or 10 nodes (Figures S1 and S2 in the supporting information).

When coupled with the more traditional composite analyses that we described prior to the SOM results, our findings suggest that the cold Atlantic characterized during pan-CONUS droughts is more of a response to La Niña conditions than an active participant in the ocean forcing. That is, La Niñas not only make the United States dry but also cool the tropical Atlantic through a well-established teleconnection (Alexander et al., 2002; Cobb et al., 2001). All else being equal, drought events that are driven by La Niña conditions would similarly be expected to select for overall cold AMO conditions arising from the tropical Atlantic response to La Niña-forcing (Seager, 2007). Hence, while our SOM analyses clearly show cold states of the Pacific to drive pan-CONUS droughts, they also suggest that the Atlantic plays a passive or ambiguous role.

4. Discussion and Conclusion

The representation of pan-CONUS droughts in the PHYDA is consistent with what is recorded in the NADA in terms of both spatial features and frequency of occurrence. This validation of the PHYDA with regard to pan-CONUS droughts supports prior validation exercises that have found the PHYDA and NADA to have strong grid-level correlations from 1500 - 2000 CE (Steiger et al., 2018) and further supports our use of the PHYDA as a new product in the current study. Regarding the ocean forcing of pan-CONUS droughts, our analysis of the PHYDA corroborates the key model-based findings in Baek et al. (2019) based on the instrumental period, namely, that pan-CONUS droughts exhibit a robust association with cold Pacific conditions but not with warm Atlantic conditions. Our analyses and those of Baek et al. (2019) thus tell a consistent story across multiple centuries about the oceanic causes of pan-CONUS droughts.

Using ensembles of SST-forced models, Baek et al. (2019) separated the contributions of internal atmospheric variability and the global ocean relative to the cumulative forcing of pan-CONUS droughts by the atmosphere and ocean and found that the contribution from the former was roughly equal to or greater than the latter. While we cannot directly assess the role of atmospheric variability in the PHYDA in the same manner it was quantified in Baek et al. (2019), we note that results of the SOM analysis are consistent with the idea that atmospheric variability plays an important role in the occurrence of pan-CONUS droughts. For instance, although our results collectively show pan-CONUS droughts to strongly prefer La Niñas, SOM 4, despite its La Niña-like conditions, demonstrates only a modest 1% increase in BMU frequency during

pan-CONUS droughts relative to non-pan-CONUS droughts. Furthermore, SOMs with El Niño conditions (i.e., SOMs 5-8) collectively claim 21% of pan-CONUS years as the BMU (Table 1). Such findings are consistent with the idea that internal atmospheric variability plays an important role in the occurrence of pan-CONUS droughts.

Our current findings are nonetheless in contrast to conventional thinking about the influence of the North Atlantic Ocean on North American hydroclimate. A key caveat of our results is that the PHYDA and the SST-forced models analyzed in Baek et al. (2019) are both based on NCAR models, the former employing the NCAR LME (Otto-Bliesner et al., 2016) in the data assimilation process and the latter being direct simulations from the NCAR CAM5. Further studies are therefore necessary to assess whether the results outlined herein and in Baek et al. (2019) are robust to model choices. This caveat notwithstanding, a potential point of reconciliation between our results and the canonical understanding of Atlantic influences, may be that the relative influences of the Pacific and Atlantic Oceans on North American hydroclimate vary over interannual and multidecadal timescales. Interannual droughts (like pan-CONUS droughts) are likely more influenced by strong ENSO variability than by the weaker SST variability in the tropical Atlantic. On decadal timescales, however, tropical Pacific and Atlantic SST variabilities are of more equal amplitude, and, when taken together with temporal persistence over this timescale, may allow the Atlantic Ocean to play a more influential role in decadal and multidecadal hydroclimate variability in North America (e.g. Cook et al., 2016; Feng et al., 2011; Nigam et al., 2011). Recent work to assess ocean forcing of multidecadal droughts in the American Southwest using the PHYDA (Steiger et al., 2019) has indeed found an Atlantic association, in which case the perceived discrepancy of the AMO's influence in the PHYDA may just be a matter of timescale.

Finally, the paleo perspective provided by our study informs future analyses seeking to understand how pan-CONUS drought risk might change into the future. To first order, projected widespread warming due to future greenhouse gas emissions and consequent increases in evaporative demand (e.g. Cook et al., 2014; Dai, 2011; Mankin et al., 2017, 2018), when coupled with projections of either reductions or modest increases in precipitation over the CONUS (Maloney et al., 2014), would portend more arid conditions over many CONUS regions (Cook, Smerdon, Seager, & Coats, 2014). In regions like the western CONUS, such enhanced aridity is projected even when vegetation responses to increased concentrations of atmospheric CO_2 are considered (Mankin et al., 2018). These biophysical and radiative responses to warming may also be joined by changes in atmospheric variability (e.g. Bishop et al., 2019; Cook et al., 2018; Singh et al., 2018) and mean-state and/or ENSO characteristics in the tropical Pacific Ocean (e.g. Cai et al., 2015; Clement et al., 1996; Coats & Karnauskas, 2017; Seager & Vecchi, 2010). Given the demonstrated strong influence of atmospheric variability and La Niña events on pan-CONUS droughts, it is thus not obvious how the frequency and intensity of these events may change in the future. Determining future risk of pan-CONUS droughts therefore requires further work on how internal atmosphere and atmosphere-ocean variability will change; how vegetation and land-atmosphere water fluxes will respond to warming, precipitation changes, and rising CO_2; and how these responses will combine with the changing mean hydroclimate to influence pan-CONUS drought occurrence.

Acknowledgments
This work was supported in part by NSF grants AGS-1243204, AGS-1401400, and AGS-1805490. The 100-member ensemble and the ensemble mean of the Paleo Hydrodynamics Data Assimilation product are publicly available at http://doi.org/10.5281/zenodo.1154913. The Living Blended Drought Atlas version of the North American Drought Atlas is publicly available at https://www.ncdc.noaa.gov/paleo-search/study/19119. The CAM5 experiments are publicly available at http://magog.ldeo.columbia.edu:81/home/.dlee/.cam5_goga/. LDEO contribution #8335. We thank two anonymous reviewers for their helpful evaluations of our manuscript.

References

Alexander, M. A., Bladé, I., Newman, M., Lanzante, J. R., Lau, N. C., & Scott, J. D. (2002). The atmospheric bridge: The influence of ENSO teleconnections on air-sea interaction over the global oceans. *Journal of Climate*, *15*(16), 2205–2231. https://doi.org/10.1175/1520-0442(2002)015<2205:TABTIO>2.0.CO;2

Andreadis, K. M., Clark, E. A., Wood, A. W., Hamlet, A. F., & Lettenmaier, D. P. (2005). Twentieth-century drought in the conterminous United States. *Journal of Hydrometeorology*, *6*(6), 985–1001. https://doi.org/10.1175/JHM450.1

Ault, T. R., George, S. S., Smerdon, J. E., Coats, S., Mankin, J. S., Carrillo, C. M., et al. (2018). A robust null hypothesis for the potential causes of megadrought in Western North America. *Journal of Climate*, *31*(1), 3–24. https://doi.org/10.1175/JCLI-D-17-0154.1

Baek, S. H., Smerdon, J. E., Seager, R., Williams, A. P., & Cook, B. I. (2019). Pacific Ocean forcing and atmospheric variability are the dominant causes of spatially widespread droughts in the contiguous United States. *Journal of Geophysical Research: Atmospheres*, *124*, 2507–2524. https://doi.org/10.1029/2018JD029219

Bishop, D. A., Williams, A. P., Seager, R., Fiore, A. M., Cook, B. I., Mankin, J. S., et al. (2019). Investigating the causes of increased twentieth-century fall precipitation over the southeastern United States. *Journal of Climate*, *32*(2), 575–590. https://doi.org/10.1175/JCLI-D-18-0244.1

Cai, W., Santoso, A., Wang, G., Yeh, S., An, S., Cobb, K. M., et al. (2015). ENSO and greenhouse warming. *Nature Climate Change*, *5*(9), 849–859. https://doi.org/10.1038/nclimate2743

Chakravarti, I. M., Laha, R. G., & Roy, J. (1967). *Handbook of methods of applied statistics* (Vol. 1). New York: John Wiley and Sons.

Clement, A. C., Seager, R., Cane, M. A., & Zebiak, S. E. (1996). An ocean dynamical thermostat. *Journal of Climate*, *9*. https://doi.org/10.1175/1520-0442(1996)009<2190:AODT>2.0.CO;2

Coats, S., Cook, B. I., Smerdon, J. E., & Seager, R. (2015). North American pancontinental droughts in model simulations of the last millennium. *Journal of Climate*, *28*(5), 2025–2043. https://doi.org/10.1175/JCLI-D-14-00634.1

Coats, S., & Karnauskas, K. B. (2017). Are simulated and observed twentieth century tropical Pacific sea surface temperature trends significant relative to internal variability? *Geophysical Research Letters*, *44*, 9928–9937. https://doi.org/10.1002/2017GL074622

Cobb, K. M., Charles, C. D., Cheng, H., & Edwards, R. L. (2003). El Niño/Southern Oscillation and tropical Pacific climate during the last millennium. *Nature*, *424*(6946), 271–276. https://doi.org/10.1038/nature01779

Cobb, K. M., Charles, C. D., & Hunter, D. E. (2001). A central tropical Pacific coral demonstrate Pacific, Indian and Atlantic decadal climate connections. *Geophysical Research Letters*, *28*(11), 2209–2212. https://doi.org/10.1029/2001GL012919

Cobb, K. M., Westphal, N., Sayani, H. R., Watson, J. T., Di Lorenzo, E., Cheng, H., et al. (2013). Highly variable El Nino-Southern Oscillation throughout the Holocene. *Science*, *339*(6115), 67–70. https://doi.org/10.1126/science.1228246

Cook, B. I., Cook, E. R., Smerdon, J. E., Seager, R., Williams, A. P., Coats, S., et al. (2016). North American megadroughts in the Common Era: Reconstructions and simulations. *Wiley Interdisciplinary Reviews: Climate Change*, *7*(3), 411–432. https://doi.org/10.1002/wcc.394

Cook, B. I., Smerdon, J. E., Seager, R., & Coats, S. (2014). Global warming and 21st century drying. *Climate Dynamics*, *43*(9-10), 2607–2627. https://doi.org/10.1007/s00382-014-2075-y

Cook, B. I., Smerdon, J. E., Seager, R., & Cook, E. R. (2014). Pan-continental droughts in North America over the last millennium. *Journal of Climate*, *27*(1), 383–397. https://doi.org/10.1175/JCLI-D-13-00100.1

Cook, B. I., Williams, A. P., Mankin, J. S., Seager, R., Smerdon, J. E., & Singh, D. (2018). Revisiting the leading drivers of Pacific coastal drought variability in the contiguous United States. *Journal of Climate*, *31*(1), 25–43. https://doi.org/10.1175/JCLI-D-17-0172.1

Cook, E. R., Seager, R., Cane, M. A., & Stahle, D. W. (2007). North American drought: Reconstructions, causes, and consequences. *Earth-Science Reviews*, *81*(1–2), 93–134. https://doi.org/10.1016/j.earscirev.2006.12.002

Cook, E. R., Seager, R., Heim, R. R. Jr., Vose, R. S., Herweijer, C., & Woodhouse, C. (2010). Megadroughts in North America: placing IPCC projections of hydroclimatic change in a long-term palaeoclimate context. *Journal of Quaternary Science*, *25*(1), 48–61. https://doi.org/10.1002/jqs.1303

Dai, A. (2011). Drought under global warming: A review. *Wiley Interdisciplinary Reviews: Climate Change*, *2*(1), 45–65. https://doi.org/10.1002/wcc.81

Enfield, D. B., Mestas-Nuñez, A. M., & Trimble, P. J. (2001). The Atlantic multidecadal oscillation and its relation to rainfall and river flows in the continental U.S. *Geophysical Research Letters*, *28*(10), 2077–2080. https://doi.org/10.1029/2000GL012745

Feng, S., Hu, Q., & Oglesby, R. J. (2011). Influence of Atlantic sea surface temperatures on persistent drought in North America. *Climate Dynamics*, *37*(3-4), 569–586. https://doi.org/10.1007/s00382-010-0835-x

Hoerling, M., & Kumar, A. (2003). The perfect ocean for drought. *Science*, *299*(5607), 691–694. https://doi.org/10.1126/science.1079053

Hu, Q., & Feng, S. (2012). AMO- and ENSO-driven summertime circulation and precipitation variations in North America. *Journal of Climate*, *25*(19), 6477–6495. https://doi.org/10.1175/JCLI-D-11-00520.1

Hu, Q., Feng, S., & Oglesby, R. J. (2011). Variations in North American summer precipitation driven by the Atlantic multidecadal oscillation. *Journal of Climate*, *24*(21), 5555–5570. https://doi.org/10.1175/2011JCLI4060.1

Hurrell, J. W., Holland, M. M., Gent, P. R., Ghan, S., Kay, J. E., Kushner, P. J., et al. (2013). The Community Earth System Model: A framework for collaborative research. *Bulletin of the American Meteorological Society*, *94*, 1339–1360. https://doi.org/10.1175/BAMS-D-12-00121.1

Kogan, F. N. (1995). Droughts of the Late 1980s in the United States as derived from NOAA Polar-Orbiting Satellite Data. *Bulletin of the American Meteorological Society*, *76*(5), 655–668. https://doi.org/10.1175/1520-0477(1995)076<0655:DOTLIT>2.0.CO;2

Kohonen, T. (1998). The self-organizing map. *Neurocomputing*, *21*(1–3), 1–6. https://doi.org/10.1016/S0925-2312(98)00030-7

Kushnir, Y., Seager, R., Ting, M., Naik, N., & Nakamura, J. (2010). Mechanisms of tropical Atlantic SST influence on North American precipitation variability. *Journal of Climate*, *23*(21), 5610–5628. https://doi.org/10.1175/2010JCLI3172.1

Liu, Y., Weisberg, R. H., & Mooers, C. N. K. (2006). Performance evaluation of the self-organizing map for feature extraction. *Journal of Geophysical Research*, *111*, C05018. https://doi.org/10.1029/2005JC003117

Lu, Z., Liu, Z., Zhu, J., & Cobb, K. M. (2018). A review of paleo El Niño-Southern Oscillation. *Atmosphere*, *9*(4), 1–27. https://doi.org/10.3390/atmos9040130

Maloney, E. D., Camargo, S. J., Chang, E., Colle, B., Fu, R., Geil, K. L., et al. (2014). North American Climate in CMIP5 experiments: Part III: Assessment of twenty-first-century projections*. *Journal of Climate*, *27*(6), 2230–2270. https://doi.org/10.1175/JCLI-D-13-00273.1

Mankin, J. S., Smerdon, J. E., Cook, B. I., Williams, A. P., & Seager, R. (2017). The curious case of projected twenty-Ffrst-century drying but greening in the American West. *Journal of Climate*, *30*, 8689–8710. https://doi.org/10.1175/JCLI-D-17-0213.1

Mankin, J. S., Williams, A. P., Seager, R., Smerdon, J. E., & Horton, R. M. (2018). Blue water trade-offs with vegetation in a CO_2-enriched climate. *Geophysical Research Letters*, *45*, 3115–3125. https://doi.org/10.1002/2018GL077051

McCabe, G. J., Palecki, M. A., & Betancourt, J. L. (2004). Pacific and Atlantic Ocean influences on multidecadal drought frequency in the United States. *Proceedings of the National Academy of Sciences of the United States of America*, *101*(12), 4136–4141. https://doi.org/10.1073/pnas.0306738101

National Climatic Data Center (2013). State of the climate: Drought–annual 2012. National Oceanic and Atmospheric Administration. Retrieved from http://www.ncdc.noaa.gov/sotc/drought/

Nigam, S., Guan, B., & Ruiz-Barradas, A. (2011). Key role of the Atlantic Multidecadal Oscillation in 20th century drought and wet periods over the Great Plains. *Geophysical Research Letters*, *38*, L16713. https://doi.org/10.1029/2011GL048650

Oglesby, R., Feng, S., Hu, Q., & Rowe, C. (2012). The role of the Atlantic Multidecadal Oscillation on medieval drought in North America: Synthesizing results from proxy data and climate models. *Global and Planetary Change*, *84-85*, 56–65. https://doi.org/10.1016/j.gloplacha.2011.07.005

Otto-Bliesner, B. L., Brady, E. C., Fasullo, J., Jahn, A., Landrum, L., Stevenson, S., et al. (2016). Climate variability and change since 850 CE an ensemble approach with the community earth system model. *Bulletin of the American Meteorological Society*, *97*(5), 735–754. https://doi.org/10.1175/BAMS-D-14-00233.1

Palmer, W. C. (1965). Meterological Drought. Research Paper No. 45.

Rasmusson, E. M., & Carpenter, T. H. (1982). Variations in tropical sea surface temperature and surface wind fields associated with the Southern Oscillation/El Niño. *Monthly Weather Review*, *110*(5), 354–384. https://doi.org/https://doi.org/10.1175/1520-0493(1982)110<0354:VITSST>2.0.CO;2

Rippey, B. R. (2015). The U.S. drought of 2012. *Weather and Climate Extremes*, *10*, 57–64. https://doi.org/10.1016/j.wace.2015.10.004
Sarachik, E., & Cane, M. A. (2010). *The El Niño–Southern Oscillation phenomenon*. Cambridge: Cambridge University Press. https://doi.org/10.1017/CBO9780511817496
Schubert, S., Gutzler, D., Wang, H., Dai, A., Delworth, T., Deser, C., et al. (2009). A U.S. Clivar project to assess and compare the responses of global climate models to drought-related SST forcing patterns: Overview and results. *Journal of Climate*, *22*(19), 5251–5272. https://doi.org/10.1175/2009JCLI3060.1
Seager, R. (2007). The turn of the century North American drought: Global context, dynamics, and past analogs. *Journal of Climate*, *20*(22), 5527–5552. https://doi.org/10.1175/2007JCLI1529.1
Seager, R., & Hoerling, M. (2014). Atmosphere and ocean origins of North American droughts. *Journal of Climate*, *27*(12), 4581–4606. https://doi.org/10.1175/JCLI-D-13-00329.1
Seager, R., Kushnir, Y., Herweijer, C., Naik, N., & Velez, J. (2005). Modeling of tropical forcing of persistent droughts and pluvials over western North America: 1856-2000. *Journal of Climate*, *18*(19), 4065–4088. https://doi.org/10.1175/JCLI3522.1
Seager, R., & Vecchi, G. A. (2010). Greenhouse warming and the 21st century hydroclimate of southwestern North America. *Proceedings of the National Academy of Sciences*, *107*(50), 21,277–21,282. https://doi.org/10.1073/pnas.0910856107
Singh, D., Ting, M., Scaife, A. A., & Martin, N. (2018). California winter precipitation predictability: Insights from the anomalous 2015–2016 and 2016–2017 seasons. *Geophysical Research Letters*, *45*, 9972–9980. https://doi.org/10.1029/2018GL078844
Steiger, N. J., Smerdon J. E. , Cook, B. I., Seager, R., Williams A. P., & Cook, E. R. (2019) Oceanic and radiative forcing of medieval megadroughts in the American Southwest. *Science Advances*, *5*, eaax0087. https://doi.org/10.1126/sciadv.aax0087
Steiger, N. J., Smerdon, J. E., Cook, E. R., & Cook, B. I. (2018). A reconstruction of global hydroclimate and dynamical variables over the Common Era. *Scientific Data*, *5*, 1–15. https://doi.org/10.1038/sdata.2018.86
Stein, K., Timmermann, A., Schneider, N., Jin, F. F., & Stuecker, M. F. (2014). ENSO seasonal synchronization theory. *Journal of Climate*, *27*(14), 5285–5310. https://doi.org/10.1175/JCLI-D-13-00525.1
Trenberth, K. E., Branstator, G. W., & Arkin, P. A. (1988). Origins of the 1988 North American Drought. *Science*, *242*(4886), 1640–1645. https://doi.org/10.1126/science.242.4886.1640
Trenberth, K. E., & Guillemot, C. J. (1996). Physical processes involved in the 1988 drought and 1993 floods in North America. *Journal of Climate*, *9*(6), 1288–1298. https://doi.org/10.1175/1520-0442(1996)009<1288:PPIITD>2.0.CO;2
Wang, J., Yang, B., Ljungqvist, F. C., Luterbacher, J., Osborn, T. J., Briffa, K. R., & Zorita, E. (2017). Internal and external forcing of multidecadal Atlantic climate variability over the past 1,200 years. *Nature Geoscience*, *10*(7), 512–517. https://doi.org/10.1038/ngeo2962
Williams, A. P., Cook, B. I., Smerdon, J. E., Bishop, D. A., Seager, R., & Mankin, J. S. (2017). The 2016 southeastern U.S. drought: An extreme departure from centennial wetting and cooling. *Journal of Geophysical Research: Atmospheres*, *122*, 10,888–10,905. https://doi.org/10.1002/2017JD027523
Wittenberg, A. T. (2009). Are historical records sufficient to constrain ENSO simulations? *Geophysical Research Letters*, *36*, L12702. https://doi.org/10.1029/2009GL038710